The Effect of Different Mn/Fe Ratio on Microstructure Alloy Based on Al-Si-Mg

D. Bolibruchova *, R. Podprocká

Department of Technological Engineering, University of Zilina,
Univerzitna 1, 010 26 Zilina, Slovak Republic
* Corresponding author. E-mail address: Danka.Bolibruchova@fstroj.uniza.sk

Abstract

This article deals with the effect of manganese that is the most applied element to eliminate the negative effect of iron in the investigated alloy AlSi7Mg0.3. In this time are several methods that are used for elimination harmful effect of iron. The most used method is elimination by applying the additive elements, so-called iron correctors. The influence of manganese on the morphology of excluded iron-based intermetallic phases was analysed at various iron contents (0.4; 0.8 and 1.2 wt. %). The effect of manganese was assessed in additions of 0.1; 0.2; 0.4 and 0.6 wt. % Mn. The morphology of iron intermetallic phases was assessed using electron microscopy (SEM) and EDX analysis. The increase of iron content in investigated alloys caused the formation of more intermetallic phases and this effect has been more significant with higher concentrations of manganese. The measurements carried out also showed that alloys with the same Mn/Fe ratio can manifest different structures and characteristics of excluded iron-based intermetallic phases, which might, at the same time, be related to different resulting mechanical properties.

Keywords: AlSi7Mg0.3 alloy, Manganese, Iron intermetallic phases, Ratio Mn/Fe

1. Introduction

Iron occurs in Al-Si alloys as an impurity. The problem arises after exceeding the critical iron content level, above which the alloy becomes brittle due to the formation of large ß-Al$_5$FeSi phase plates. Depending on the chemical composition of the alloy, we can calculate the so-called critical value of Fe$_{krit}$ in wt. % using the equations [1, 2]:

$$Fe_{crit} \approx 0{,}075 \; x \; (wt. \; \% \; Si) - 0{,}05 \qquad (1)$$

The main structural consequence of the presence of iron in aluminium alloys is the presence of intermetallic compounds, in particular in the form of ß-Al$_5$FeSi phase that is excluded in the unfavourable needle/platelet morphology [3].

The formation of iron-based intermetallic phases depends on cooling rate, eutectic modification, and on manganese content in the alloy. Depending on these factors, also the morphology changes of the excluded phases – from needle/platelet of ß-Al$_5$FeSi phase to skeletal particles or the so-called Chinese characters of α-Al$_{15}$(Fe,Mn)$_3$Si$_2$ phase that affect the mechanical properties. The maximum permissible amount of iron in primary alloys is about 0.15 wt. %. However, the amount can be more than 1 wt. % in case of secondary recycled alloys. The higher the amount of iron in the alloy, the greater the amount of intermetallic iron-based phases in the material, and there may occur a serious decrease in the mechanical properties of the alloy – especially the reduced elongation and tensile strength [4, 5].

In technical practise, such alloys based on Al-Si-Mg or Al-Si-Cu are used for the production of castings, where the presence of other elements provides a space for the formation of intermetallic compounds. For the above reasons, correctors are used to reduce the negative influence of iron in secondary alloys. Such correctors may cause a change in the morphology of iron-based intermetallic

phases, which may lead to improved properties of the alloy. In practice, manganese is most commonly used for this purpose [6, 7].

Manganese is an effective element in influencing iron-based needle-like intermetallic phases. However, the addition of manganese to alloys with high iron and chromium content may cause the formation of the so-called sludge phases that cannot be removed from the alloy by conventional metallurgical processes or methods [1]. The alloy tendency to form sludge phases depends on the content of iron, manganese and chromium, and it is given by the so-called "sludge" factor (SF) [8]:

$$SF = 1 \% \ Fe + 2 \% \ Mn + 3 \% \ Cr \qquad (2)$$

According to the recommendations of several literary sources [e.g. 5], manganese is used in the Mn/Fe ratio = 0.5 to reduce the negative effect of iron, but for some castings the Mn/Fe ratio > 0.7 is required. The recommended amount of addition is ambiguous according to current research [9, 10].

2. Methodology of experiments

The material AlSi7Mg0.3 alloy has been chosen as the experimental material. The chemical composition of the investigated alloy is shown in Tab. 1.

In this alloy, the effect of manganese was analyzed on the elimination of the adverse effect of iron. In the initial steps of the experiment we determined the desired concentration of iron when crystallisation of harmful intermetallic phases occurs. For this purpose, we prepared secondary alloys with different iron contents: 0.4; 0.8 and 1.2 wt. %.

Samples with the weight approximately 300g with different iron contents were used to prepare an alloy where we altered the amount of manganese. Manganese was proposed as the corrector of iron intermetallic phases. It was added in amounts of 0.1; 0.2; 0.4 a 0.6 wt. %. The chemical composition of the secondary alloys with corresponding manganese contents is shown in Tab. 2.

According to (1) there is an adverse effect of iron after exceeding the so-called critical iron content value. Therefore, we calculated critical iron content value for each alloy. The critical iron content values for each alloy are shown in Tab.3. In the investigated alloy we intentionally increased the concentration of iron above the value permitted by EN 1706 standard, and above the critical iron content value calculated according to (1). The purpose was to create, in the microstructure, large iron-based intermetallic phases that were subjected to the effect of a corrector.

Another important aspect to be taken into account when using recycled aluminium alloys and when adding manganese to alloys is the concentration of iron, manganese and chromium. With the increasing content of these elements, the alloy has a higher tendency to form sludge formations in the alloy structure. The segregation (sludge) factor, which indicates how many of these formations will form, was calculated for each alloy based on Formula (2). The calculated sludge factor values are shown in Tab. 3.

Table 1.
Chemical composition of the experimental alloy AlSi7Mg0.3

Elements	Si	Fe	Mn	Mg
(wt. %)	7.093	0.099	0.072	0.38
Elements	Cr	Ti	Sr	Al
(wt. %)	0.002	0.18	0.015	92.14

Table 2.
Chemical composition of the secondary alloys AlSi7Mg0.3 after the addition of Mn

Alloy	Si	Fe	Mn	Mg	Cr	Ti	Sr	Al	Mn/Fe
A1	6.889	0.339	0.149	0.348	0.002	0.0039	0.0077	92.05	0.44
A2	6.892	0.343	0.263	0.348	0.002	0.004	0.0082	91.95	0.77
A3	6.673	0.347	0.408	0.308	0.002	0.0051	0.0020	92.23	1.18
A4	6.583	0.345	0.677	0.352	0.0032	0.0046	0.0091	91.82	1.96
B1	6.732	0.779	0.183	0.354	0.002	0.160	0.011	91.76	0.23
B2	6.245	0.778	0.231	0.332	0.002	0.166	0.0099	92.22	0.30
B3	6.353	0.731	0.334	0.3000	0.002	0.0031	0.0020	92.24	0.46
B4	6.111	0.781	0.656	0.296	0.003	0.0028	0.0020	92.12	0.84
C1	6.344	1.138	0.110	0.302	0.002	0.153	<0.0020	91.93	0.10
C2	6.205	1.198	0.330	0.334	0.0024	0.148	0.0095	91.75	0.28
C3	6.011	1.110	0.347	0.290	0.002	0.0029	0.0020	92.21	0.31
C4	5.929	1.129	0.538	0.283	0.0027	0.0030	0.0020	92.09	0.48

Table 3.
Calculated values of Fe_{crit} and SF for secondary alloys AlSi7Mg0.3 after the addition of Mn

ALLOY	Fec$_{crit}$ [%]	SF	ALLOY	Fec$_{rit}$ [%]	SF	ALLOY	Fe$_{crit}$ [%]	SF	ALLOY
A1	0.339	0.643	**B1**	0.779	1.151	**C1**	1.138	1.364	**A1**
A2	0.343	0.875	**B2**	0.778	1.246	**C2**	1.198	1.865	**A2**
A3	0.347	1.169	**B3**	0.731	1.405	**C3**	1.110	1.810	**A3**
A4	0.345	1.708	**B4**	0.781	2.102	**C4**	1.129	2.213	**A4**

In the samples, we assessed the effect of manganese at varying iron contents and the Mn/Fe ratios on the morphology of iron-based excluded phases. Higher iron content in the alloy was achieved by adding AlFe10 pre-alloy. Manganese was added to the alloy in the form of AlMn20 pre-alloy. Iron and the corrector (manganese) were added to the melt with temperature 780 ± 5 °C. This higher temperature was chosen due to thorough and consistent melting of the pre-alloy. Melting of each alloy was carried out in an electric resistor furnace with a T15 regulator, and in a graphite crucible treated with a protective coating. In the metallurgical process, we did not affect the alloys – they were not inoculated, modified or refined whatsoever. However, it should be pointed out that the primary alloy already contained Ti (0.18 wt. %) and Sr (0.015 wt. %), therefore this alloy can be considered pre-inoculated and pre-modified by the primary manufacturer.

As part of the metallurgical processes, we only stirred the alloy and removed the oxidic film from the melt surface. The samples were cast into a metallic mould heated to 200 ± 5 °C. All alloys were cast at 760 ± 5 °C.

3. Results and discussion

In the structure of the A1 sample (Fig. 1a) with 0.4 wt. % Fe and 0.1 wt. % Mn and at the mutual Mn/Fe ratio = 0.44, the alloy structure mainly features needle-like particles of small dimensions that are locally present in the form of smaller plates. At the same time, increasing the manganese content to 0.2 wt. % resulted in observable ß-Al$_5$FeSi plate fragmentation in the A2 alloy structure at the Mn/Fe ratio = 0.77 (Fig. 1b). The increased Mn/Fe ratio also contributed to a change in the ß-Al$_5$FeSi phase morphology to the shape of smaller skeletal formations. The observed presence of increased manganese content together with Fe and Si elements also confirmed in alloys A3 a A4 (Fig. 1c, d), that it is the α-Al$_{15}$(Fe,Mn)$_3$Si$_2$ phase (Fig. 2). The ß-Al$_5$FeSi phase is still present in the form of smaller plates. Despite the relatively high ratio in alloys with higher concentrations of Mn (A3, A4), no sludge formations were identified in the microstructure.
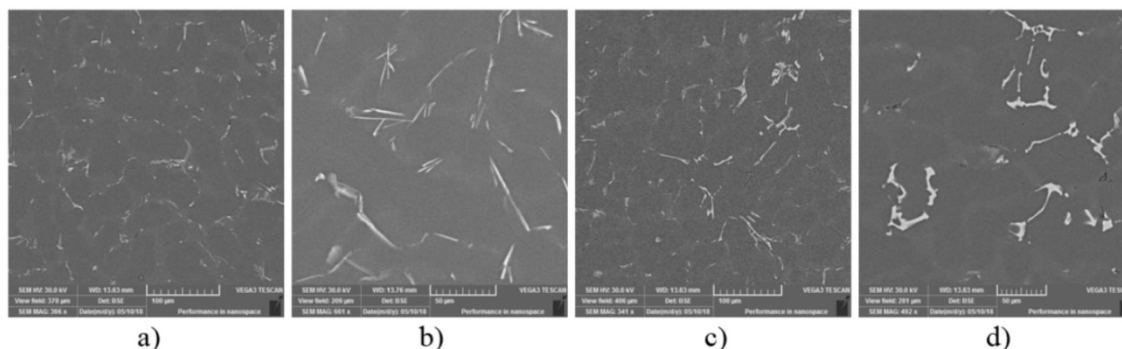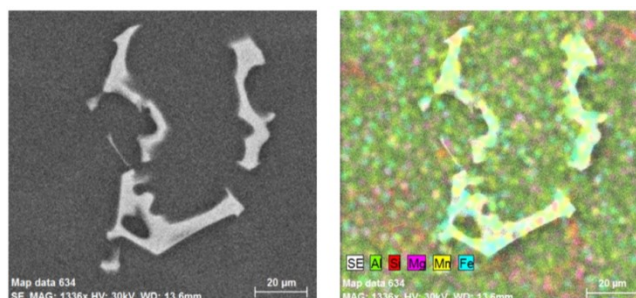

Fig. 1. SEM images of investigated alloys: a) A1, Mn/Fe = 0.44; b) A2, Mn/Fe = 0.77; c) A3, Mn/Fe = 1.18; c) A4, Mn/Fe = 1.96

Fig. 2. Mapping of skeletal particle Al$_{15}$(FeMn)$_3$Si$_2$ phase of the secondary A4 alloy a) SEM b) Mapping

After increasing the iron content to 0.8 wt. % and adding 0.1 wt. % of manganese, the B1 alloy structure manifests the presence of iron-based intermetallic phases excluded in the form of long needles (Fig. 3a). In the case of the B2 alloy, there are still needle-

like morphology particles present in the structure of the alloy (Fig. 3b). In the needle-like particle we identified, in particular, Si, Fe and Mn elements, while manganese content was low, which

did not result in a change in the morphology of the ß-Al₅FeSi phase (Fig. 4). The change in the ß - Al₅FeSi intermetallic phase morphology was observed in the B3 alloy, with the presence of the ß-Al₅FeSi intermetallic phase, but in a smaller amount and size compared to the previous alloys (Fig. 3c). A larger amount of phases with more suitable morphologies

excluded in the form of skeletal formations or Chinese characters occur in the B4 alloy with 0.6 wt. % Mn and Mn/Fe ratio = 0.84. The SEM picture (Fig. 3d) shows that skeletal formations are excluded in a more compact shape as in alloys with 0.4 wt. % iron, and when compared to the B3 alloy.
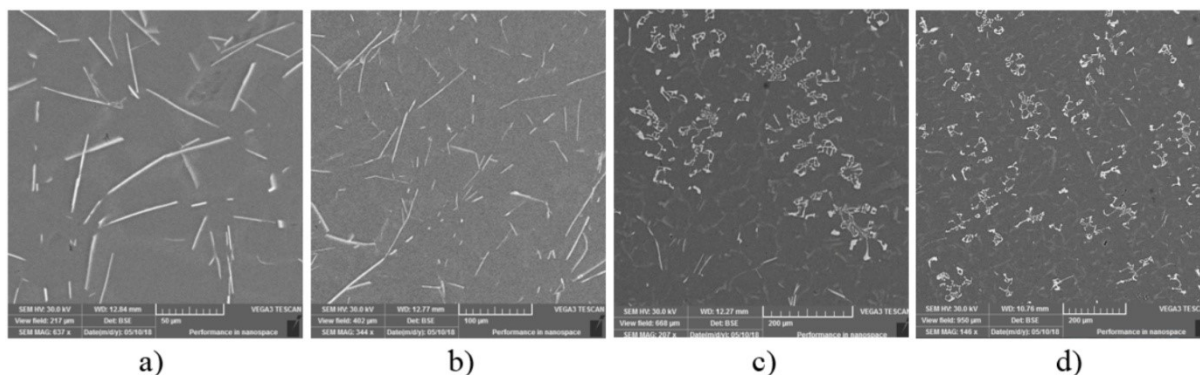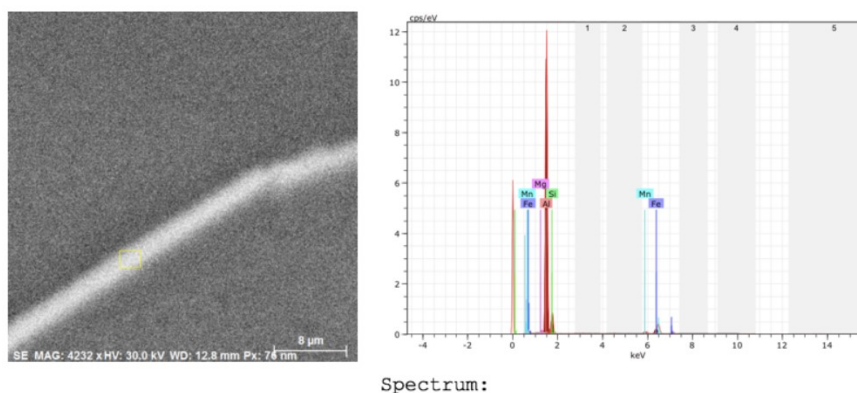

a)   b)   c)   d)

Fig. 3. SEM images of investigated alloys: a) B1, Mn/Fe = 0.23; b) B2, Mn/Fe = 0.30; c) B3, Mn/Fe = 0.46; c) B4, Mn/Fe = 0.84

Spectrum:

Element	Series	unn. C [wt.%]	norm. C [wt.%]	Atom. C [at.%]	Error (3 Sigma) [wt.%]
Aluminium	K-series	70.66	75.17	78.95	11.44
Silicon	K-series	15.11	16.08	16.22	3.39
Iron	K-series	5.63	5.99	3.04	1.29
Manganese	K-series	2.07	2.20	1.14	0.75
Magnesium	K-series	0.53	0.56	0.65	0.39
	Total:	94.00	100.00	100.00	

Fig. 4. EDX analysis of needle particles β - Al₅FeSi phase in B2 alloy

In the alloy structure, there are only iron-based intermetallic phases of a needle-like morphology (Fig. 5a) occurring at the highest iron content and manganese addition of 0.10 wt. %. at the highest iron content and manganese addition of 0.10 wt. %, and the mutual Mn/Fe ratio = 0.10, the increased manganese content by 0.2 wt. % only partially contributed to changes in the morphology. In addition to a partial elimination of ß-Al₅FeSi, the alloy structure also featured a smaller amount of skeletal

formations (Fig. 5b). SEM pictures of the C3 and C4 alloys exhibit equally distributed ß-Al₅FeSi phase formations in the form of plates and a smaller amount of skeletal formations of small dimensions (Fig. 5c, d). The EDX analysis proved that skeletal and plate formations were formed by Si, Fe and Mn elements. Higher manganese content was identified in both alloys in the particles of skeletal morphology (Fig. 6).
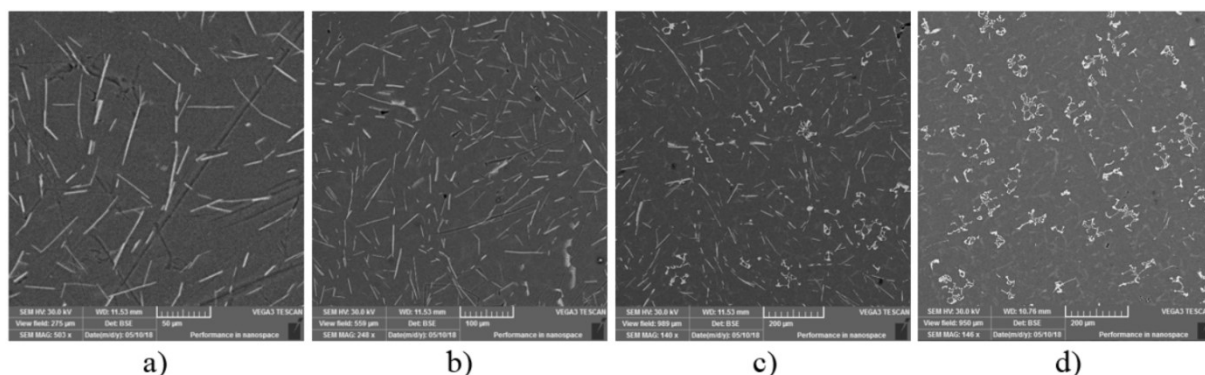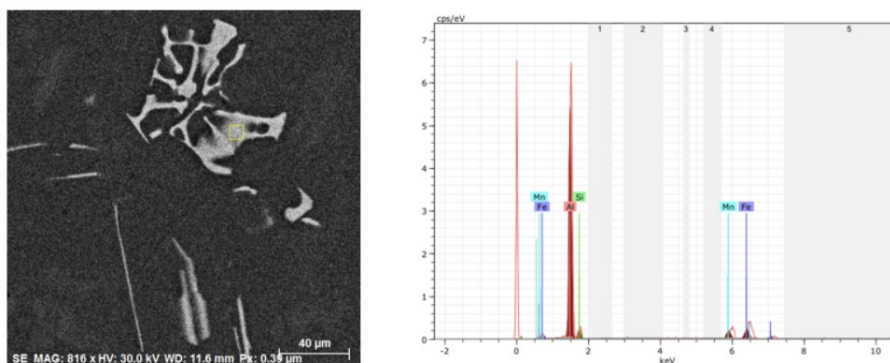
Fig. 5 SEM images of investigated alloys: a) C1, Mn/Fe = 0.10; b) C2, Mn/Fe = 0.28; c) C3, Mn/Fe = 0.31; c) C4, Mn/Fe = 0.48

Spectrum:

Element	Series	unn. C [wt.%]	norm. C [wt.%]	Atom. C [at.%]	Error (3 Sigma) [wt.%]
Aluminium	K-series	57.71	76.86	82.73	9.50
Silicon	K-series	7.57	10.08	10.43	2.12
Iron	K-series	5.55	7.39	3.85	1.07
Manganese	K-series	4.25	5.66	2.99	0.89
	Total:	75.09	100.00	100.00	

Fig. 6 EDX analysis of skeletal particle $Al_{15}(FeMn)_3Si_2$ phase in C3 alloy

Tab. 4 shows the measured average lengths and the predominantly occurring morphology of excluded intermetallic phases in the investigated alloys. As the iron content increased in every consecutive alloy, we observed formation of more intermetallic phases. The influence of iron is more significant in alloys with a higher manganese concentration. As can be seen in Tab. 4, the size of intermetallic compounds increases with iron and manganese contents. In alloys containing 0.4 wt. % iron, and 0.1 + 0.3 wt. % Mn, intermetallic compounds are present in the form of needles or plates. The change in the morphology only occurs at the Mn/Fe ratio > 1.18. At a higher Fe content (approximately 0.8 wt. %), the occurrence of skeletal formations or Chinese characters begins at a Mn/Fe ratio lower than in the case of the alloy containing Fe 0.4 wt. %. In the alloys containing the highest amount of Fe, and containing Mn 0.4 a 0.6, the predominating phase is α-$Al_{15}(FeMn)_3Si_2$ at a relatively low Mn/Fe ratio compared to alloys with lower Fe contents.

5. Conclusions

The formation and characteristics of intermetallic phases in the AlSi7Mg0.3 alloy is dependent on the iron content ratio to manganese (Mn/Fe). The effect of iron associated with the morphology of the excluded phase is enhanced with increased manganese content. The size and number of intermetallic phases grow with increasing iron content as well as manganese content in the alloy. At an equal mutual Mn/Fe ratio = 0.45, in the alloy with 0.4 wt. % iron the microstructure consists of smaller plate or needle particles, and at 0.8 and 1.2 wt. % Fe skeletal formations or Chinese characters are dominantly present. A similar effect can be observed also at Mn/Fe ratio = 0.8, where at lower iron content plate formations are excluded, and at 0.8 wt. % Fe content the structure is mostly composed of Chinese characters.

Table 4.
Morphology of intermetallic phases in investigated alloys

ALLOY Mn/Fe	LENGTH [µm]	PHASE MORPHOLOGY	ALLOY Mn/Fe	LENGTH [µm]	PHASE MORPHOLOGY	ALLOY Mn/Fe	LENGTH [µm]	PHASE MORPHOLOGY
A1 *0.44*	19.96	*needles or plates* (β-Al$_5$FeSi)	**B1** *0.23*	40.75	*needles* (β-Al$_5$FeSi)	**C1** *0.10*	31.66	*needles* (β-Al$_5$FeSi)
A2 *0.77*	24.15	*needles or plates* (β-Al$_5$FeSi)	**B2** *0.30*	46.95	*needles* (β-Al$_5$FeSi)	**C2** *0.28*	49.21	*needles* (β-Al$_5$FeSi) or *Chinese script* (αAl$_{15}$(FeMn)$_3$Si$_2$)
A3 *1.18*	24.20	*skeletal particles* (α-Al$_{15}$(FeMn)$_3$Si) *or plates* (β-Al$_5$FeSi)	**B3** *0.46*	41.67	*skeletal particles* (αAl$_{15}$(FeMn)$_3$Si$_2$)	**C3** *0.31*	40.95	*needles* (β-Al$_5$FeSi) or *Chinese script* (αAl$_{15}$(FeMn)$_3$Si$_2$)
A4 *1.96*	22.17	*plates* (β-Al$_5$FeSi)	**B4** *0.84*	44.80	*skeletal particles* or *Chinese script* (αAl$_{15}$(FeMn)$_3$Si$_2$)	**C4** *0.48*	75.73	*skeletal particles* or *Chinese script* (αAl$_{15}$(FeMn)$_3$Si$_2$)

Based on the above it can be concluded that in an alloy with a higher iron content and the same Mn/Fe ratio compared to an alloy with a lower content there is a higher assumption of formation of skeletal formations or Chinese characters. The effect of manganese on the characteristics and amount of excluded phases grows with increasing iron content in the alloy. At a relatively equal Mn/Fe ratio, phases of the same or similar morphology do not have to be formed. Another criterion that was taken into account when reducing the adverse effect of iron by manganese were sludge phases. The susceptibility of the melt to the formation of these hard intrusions increases with growing content of manganese, iron and chromium in the alloy. The results of the sludge factor (SF) calculation in the investigated alloys did not confirm the occurrence of these phases despite the relatively high SF in alloys with the highest iron content. However, it may be assumed that the further increase in manganese content may result in the formation of sludge phases.

Acknowledgement

References

[1] Taylor, J.A. (2012). Iron-containing intermetallic phases in Al-Si based casting alloys. *Procedia Materials Science.* 1, 19-33.

[2] Shabestari, S.G. (2004). The effect of iron and manganese on the formation of intermetallic compounds in aluminium-silicon alloys. *Materials Science and Engineering.* 383(2), 289-298.

[3] Dinnis, C. (2005). As-cast morphology of iron-intermetallics in Al-Si foundry alloys. *Scripta Materialia.* 53(8), 955-958.

[4] Podprocká, R. & Bolibruchová, D. (2017). Iron intermetallic phases in the alloy bBased on Al-Si-Mg by applying manganese. *Archives of Foundry Engineering.* 17(3), 217-221.

[5] Cao, X. & Campbell, J. (2006). Morphology of Al$_5$FeSi Phase in Al-Si Cast Alloys. *Materials Transactions.* 47(5), 1303-1312.

[6] Khalifa, W., Samuel, F.H. & Gruzleski J.E. (2005). Nucleation of Fe-intermetallic phases in the Al–Si–Fe alloys. *Metall. Mater. Trans.* A 36A, 1017-1032

[7] Matejka, M. Bolibruchová, D. (2018). Effect of remelting on microstructure of the AlSi9Cu3 alloy with higher iron content. *Archives of Foundry Engineering.* 18(4), 25-30.

[8] Ferraro, S., Fabrizi, A. & Timelli, G. (2015). Evolution of sludge particles in secondary die-cast aluminium alloys as function of Fe, Mn and Cr contents. *Materials Chemistry and Physics.* 153, 168-179.

[9] Mrówka-Nowotnik, G., Sieniawski, J. & Wierzbińska, M. (2007). Intermetallic phase particles in 6082 aluminium alloy. *Archives of Materials Scienceand Engineering.* 28(2), 69-76.

[10] Vasková, I., Conev, M. & Hrubovčáková, M. (2018). Technological properties of moulding sands with geopolymer binder for aluminum casting. *Archives of Foundry Engineering.* 18(4), 45-49.